EPJ Web of Conferences **114**, 02148 (2016)
DOI: 10.1051/epjconf/201611402148


# Air flow phenomena in the model of the blind drift

Marek Jaszczur[1,a], Michał Karch[1], Marcin Zych[1], Robert Hanus[2], Leszek Petryka[1] and Dariusz Świsulski[3]

[1]*AGH University of Science and Technology, 30-059 Krakow, Poland*
[2]*Rzeszow University of Technology, 35-959 Rzeszow, Poland*
[3]*Gdansk University of Technology, 80-233 Gdansk, Poland*

**Abstract.** In the presented paper, Particle Image Velocimetry (PIV) has been used to investigate flow pattern and turbulent structure in the model of blind drift. The presented model exist in mining, and has been analyzed to resolve ventilation issues. Blind region is particularly susceptible to unsafe methane accumulation. The measurement system allows us to evaluate all components of the velocity vector in channel cross-section simultaneously. First order and second order statistic of the velocity fields from different channel cross-section are computed and analyzed.

## 1 Introduction

The researchers from AGH University of Science and Technology (traditional university name is AGH Mining and Metallurgy) in the last few decades carried out large number of studies related to the safety and comfort of people working in extremely difficult climatic conditions that occur in underground mines [1,2]. One of the most important element of this research are issues related to ensuring proper ventilation in the people workplace. In order to ensure the ventilation designers should have the knowledge, experience and tools that will help solve emerging questions and problems [3-6]. Proper ventilation requires good knowledge about velocity field in blind drift [7-8]. Maintained for technological reasons, the blind chamber is exposed particularly to dangerous accumulations of methane. A methane-air mixture flows into the cave from a goaf space. This flow is not limited, because it should push away the zone of high methane concentrations from the conveyor drive located at the terminal section of the wall. The existing system of duct connections causes this to be the least intensively ventilated part of the typical longwall.

In literature there are only few experimental studies related to similar topics. Most of works concentrate on numerical analysis [9-12] in which depending on the considered variant of the exploitation system, various numerical models has been tried and tested for the best way to reproduce the real flow. In order to use any new or existing turbulence model, this model has to be validated base on theory, experimental measurement based on real or laboratory scale model [13-14].

In the typical copper mines chamber-pillared system has been used. The chamber is ventilated by fans placed at the inlets. The length of the chambers is typically 25-30 m, in some cases ventilated chamber length up to 60 m. The geometry investigated in this study differs significantly from those analyzed in literature. It arranges the connections between the main ventilation ducts and separately ventilated bind chamber.

[a] Corresponding author: marek.jaszczur@agh.edu.pl

## 2 Experimental setup

The experimental model of the blind drift set-up is shown in figure 1. It is assumed, that dimensions of the real object are: the blind drift 4 m x 2 m, and the length of the blind drift is 20 m. The main fan diameter is 0.8 m. The geometrical scale of the physical model is 1:10.

The outlet of the fan has been installed 15 cm from the beginning of the channel. In real flow the Reynolds number (base on the hydraulic diameter and mean velocity) excess of 100 000.

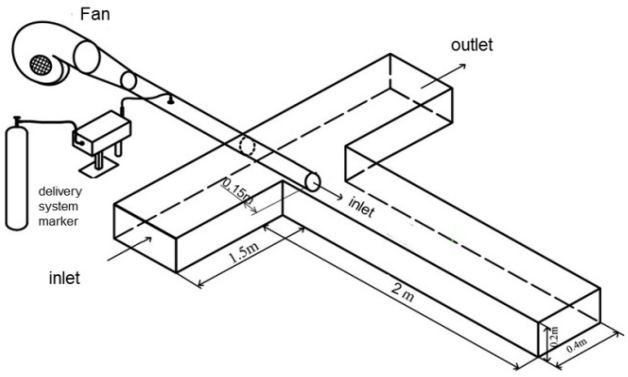


**Figure 1.** Experimental set-up of the blind drift.

Measurements were performed for the average airflow velocity in the inlet duct equal 35.4 m / s, which gives a Reynolds number of about 180 000.

In order to stabilize the air jet and to obtain the axisymmetric flow velocity profile downstream from the fan, a 1.35 m jet-stabilized section was provided. This

section comprised a diffuser, a confuser and a pipe 0.2 m in diameter with a force-mode fan at the inlet. The channel was made entirely of plexiglas (but in some cases side and bottom walls were cover by real stones to make the wall more realistic - see figure 4) to meet the requirement of transparency which is imposed by the selected method of measurement.

## 3 Measurement

Particle Image Velocimetry (PIV) and Stereoscopic –PIV method was used to evaluate the velocity vector components [15].

Velocity measurement in this method is based on a statistical estimate of the particle motion marker mixed with the air in the measurement area [16]. The seeding for the PIV method was DEHS oil sprayed through an atomiser, to obtain a particle diameter of about 1 μm. The seeding particles were introduced to the inlet air stream, immediately behind the flow-stabilizing section. During the measurement, the test area was illuminated with a laser beam (ie. the knife light). Particles injected to the flow works as a tracer particles and reflect laser light. Reflected light is recorded by a CCD camera placed perpendicular (or in the same of stereoscopic measurement inclined) to the plane of the light. In order to determine the distribution of the velocity field of the flow, tracer particles are recorded by the camera on two frames. The measuring equipment was subjected to testing and calibration procedures under flow condition to yield the accurate statistics. The Davis software ver. 8.0 [17] was used to analyze the images to evaluate the velocity vector components as well as other statistics.

Measuring section is presented in figure 2. The particles were illuminated with a double-pulse Nd:YAG laser of energy of about 60 mJ per pulse. The digital images were acquired by 4 Mpx monochromatic CCD camera.

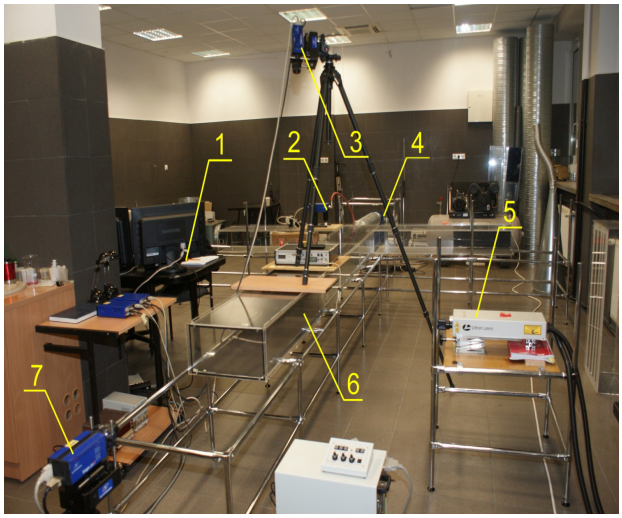


**Figure 2.** The photo of a measuring section: 1-measuring computer, 2-seeds system, 3-camera no.1, 4-centrifugal fan, 5- double-pulse Nd:YAG laser, 6-blind drift, 7-camera No. 2.

In each experiment, up to 1000 double frame images were recorded with the camera recording at a frequency of 5-7 Hz, which resulted in an overall time of one measure of around 3 minutes. Time $\Delta t$ between two subsequent frames varied from about 20 μs to 200 μs. However, the measurements at the end of the blind drift were taken in the range of 3000-4000 μs, because (in some cases) the velocities there were much lower than in the other sections. During the calculations, the size of interrogation windows that exhibit satisfying results was not constant but varied from 16x16 to 64x64 pixels.

All fan arrangements in the model blind drift study in this paper are presented in the figure 3. In the first case (1) the fan tube is parallel to the canal walls and the distance between the axis of the fan and the top and left wall was 5 cm. In the case (2) the fan tube is also parallel to the channel walls but the distance between was 8 cm.

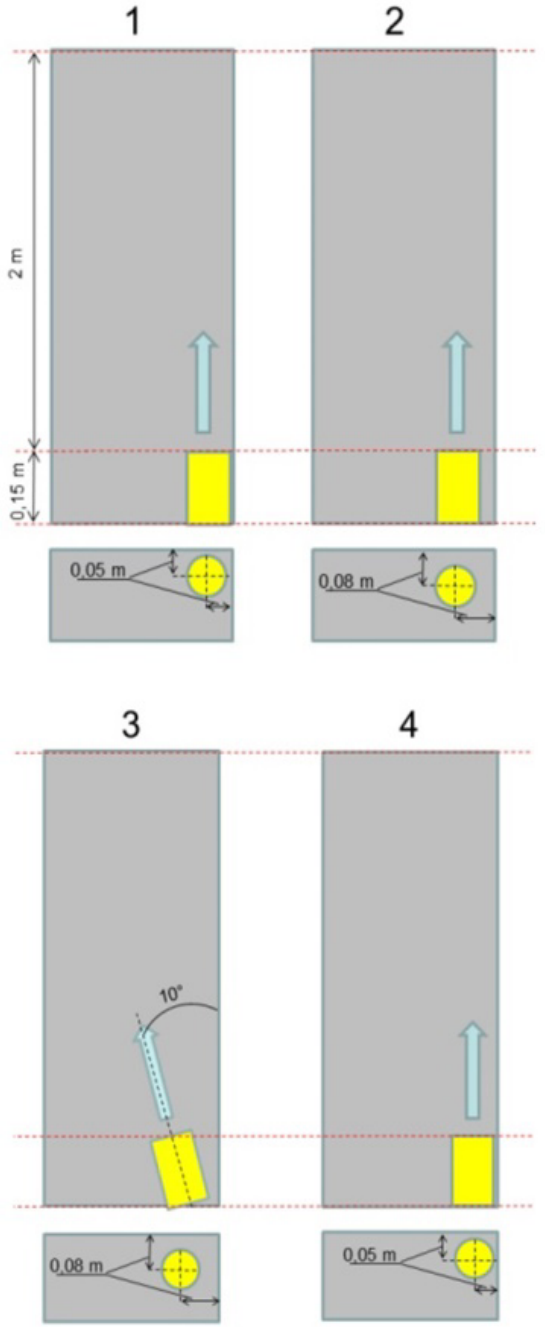


**Figure 3.** Schematic diagram of four different fan outlet location and inclination in the model of the blind drift.

For case (3) the fan tube is inclined with an angle of 10 degrees to the side wall of the channel and located as for case (2). Case (4) - fan is set parallel to the channel walls. The distance between the axis of the fan and the rough wall was 5 cm. For cases (1)-(3) all channel walls were smooth while in case (4) two of four walls have a high wall roughness (see figure 4).

The high wall roughness was obtained using real small size stones. Size of applied stones contain from 1 to 1.5 cm. The use of walls with high surface roughness was to bring actual conditions in the blind drift.

**Figure 4.** The channel with two walls with a high roughness.

As was mentioned, only in the first case, the air flow stream goes to the end of the channel parallel to the wall. In the other three settings the air flow stream breaks away from the wall and turns toward the opposite wall. In the current research optimal position and inclination has been evaluated in order to get correct and efficient ventilation of the blind drift.

## 4 Results

Contours of steam-wise velocity component in the blind drift for all cases considered here is presented in figure 5 in the x-y cross section located in the axis at the fan (high equal to the fan tube axis position). It is interesting to compare the results obtained for case (1) and (4) for which fan tube is located in the same place but the channel walls are smooth or have high wall roughness. Qualitative difference is observed between velocity fields obtained from these two scenarios. In case (4), when the walls are rough main flow stream turned into the opposite wall. Flow pattern for case (4) is similar to case (3) where fan tube is inclined and main flow stream in a natural way turned left.

Figures 6-8 shown profiles of the stream-wise velocity component along the channel horizontal line at the axis fan and for y = 30 cm from the fan outlet.

Figure 6 shows the measured velocity for cases (1), (3) and (4) at the distance y = 30 cm from the fan outlet. The main flow stream of air is directed at an angle for case (3). Velocity distributions obtained from cases (1) and (4) are similar. Velocity distributions obtained from case (3) is shifted to the left wall.

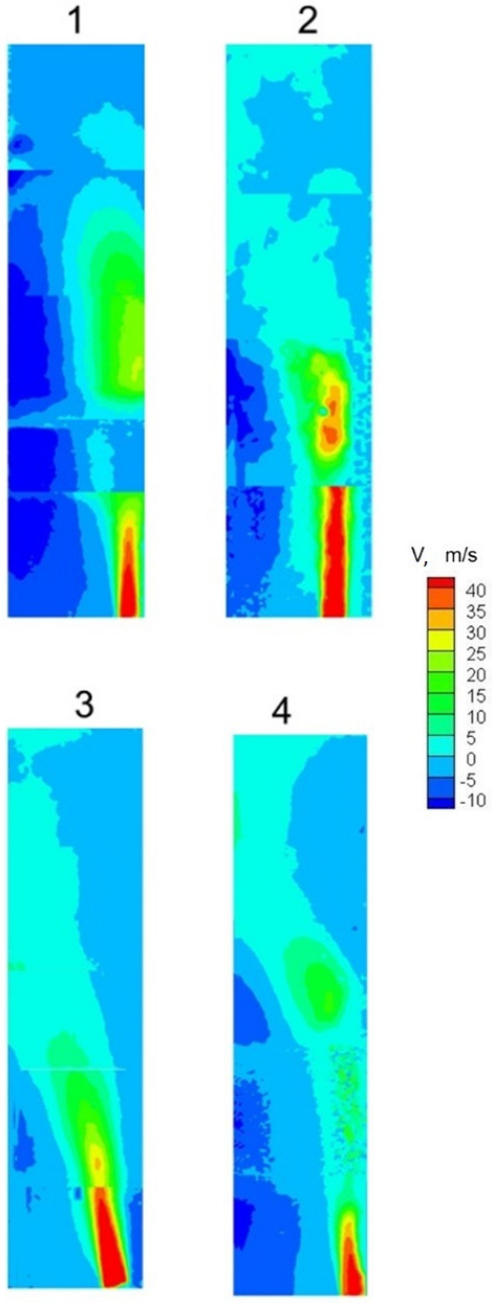


**Figure 5.** Contours of stream-wise velocity in the blind drift in the x-y cross section.

Figure 7 shows the measured velocity for case (1) and (4) at a distance y = 80 cm from the fan outlet. At this point, you can see that in case (4) (the walls are rough) air flow main stream begins to turn toward the opposite wall. There is slight difference (about 0.5 m / s) between maximum velocities for presented cases.

Figure 8 shows the measured velocity in case 3 in at a distance of 120 cm from the fan outlet. Figures 5 (bottom) show a reversal of the air flow in the duct. Such a situation occurred in all cases studied, except case 1. For different settings of the fan turning air stream in the direction of the opposite wall is followed at different points in the channel. It can be seen in figure 5.

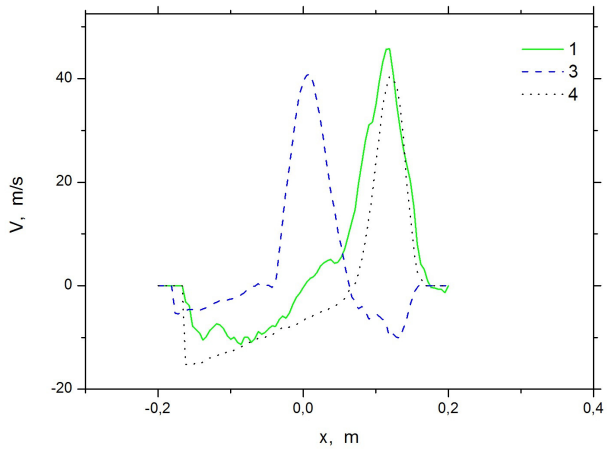


**Figure 6**. Flow stream-wise for the cases (1), (3) and (4) at a distance y = 30 cm from the fan outlet.

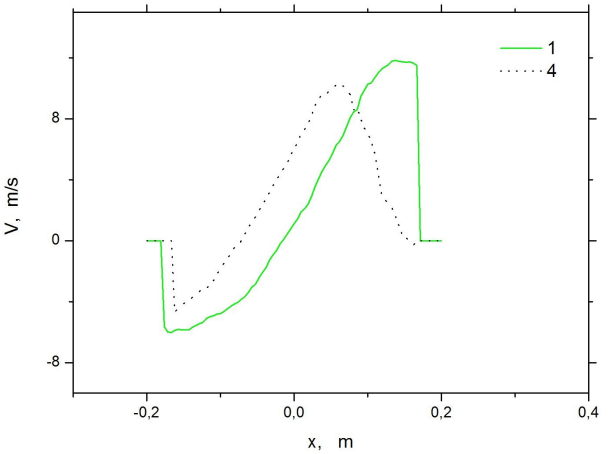


**Figure 7**. Flow stream-wise for the cases (1), (4) at a distance y = 80 cm from the fan outlet.

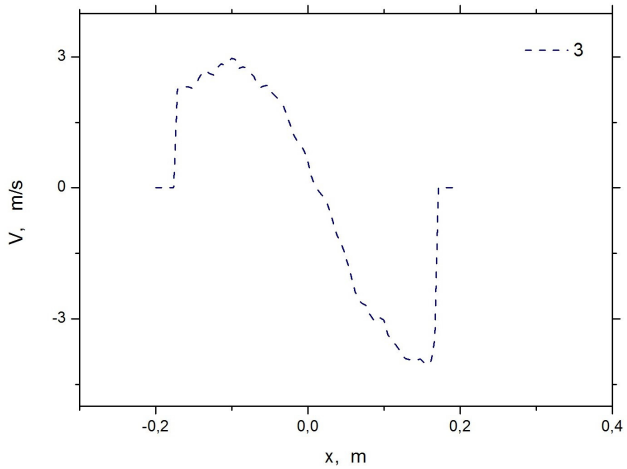


**Figure 8**. Flow stream-wise for the cases (3) at a distance y = 120 cm from the fan outlet.

Figure 9 shows flow fields obtained for case (1) and (3). The flow field is shown in the x-z cross-section plane of the channel. This data has been obtained using stereoscopic measurement which allow to determine all velocity vectors components.

In figure 9, the presented measurement was taken at a distance of 30 cm counted from the end of the channel. As can be seen for case (1) main air flow stream hits the end wall while for case (4) situation is different and largest positive velocity is observed close to the left wall and negative velocity close to the right wall. This is related to the large recirculation areal existing at the end of the blind drift which directly influence ventilation processes.

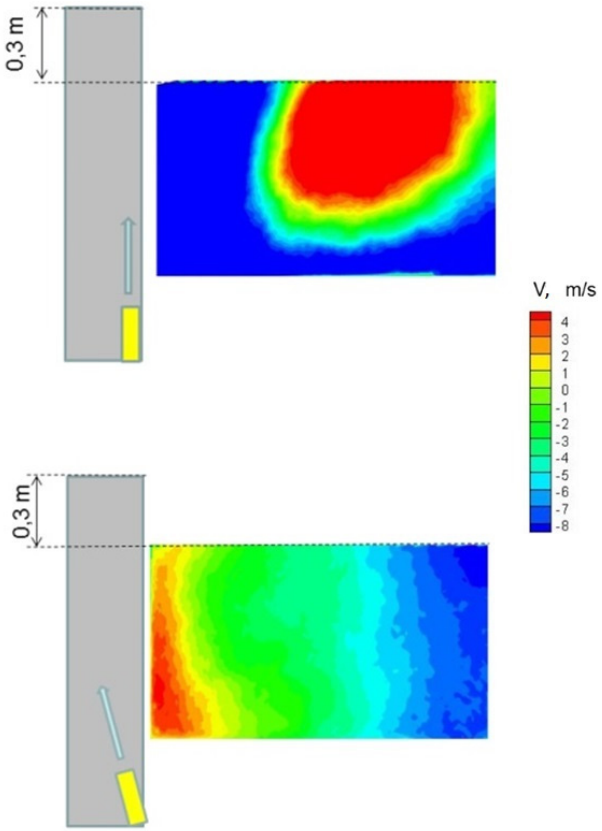


**Figure 9.** The velocity flow field obtained in the cave using 3D stereoscopic measurement (Stereo-PIV) in the x-z cross section at the distance 30 cm from the channel end.

Figure 9 also shows, that in case (1) when the axis of the fan tube is at a distance of 5 cm from the channel walls the main flow stream of air is not reversing before it reach the end of the channel. While the fan tube is set at an angle of 10 degrees as for the case (3) the air flow is fully reversed and the zone of negative stream-wise velocity component covers right part of the channel (at presented distance). It is also worth to notice, that in case (3) the area with velocity close to or equal 0 m / s (no air movement) is bigger than for case 1. This may also suggest, that this area may be less ventilated.

## 5 Conclusions

In this paper preliminary measurement of velocities in blind drift result are presented. Roughness and angle of fan have influence on velocity fields in the blind chamber. The laboratory setup represents a simplified model of the crossing of longwall with ventilation gallery. Despite of the simple geometry of the flow

domain, the structure of the velocity field is very complex. The examined flow is characterized by such flow features as separation, air stream impingement on the wall, stress-driven flow and strong streamline curvature.

Depending on the configuration, one large or two small zones with recirculating flow can be distinguished in the flow due to the shape of the velocity field created by the inlet air jet. This directly influences ventilation processes at the end of the blind drift. In the case when one large vortex exists, the whole cavity is well ventilated and fresh air is delivery to the end wall. When the flow forms two separated recirculation zones or two partially mixed zones as in case (3) and case (4) the ventilation conditions become much worse and only a small or very small amount of primary fresh air is delivery to the end of cavity.

Stereoscopic PIV offers a good insight into ventilation processes in the blind drift aired with jet fans. The system is able to capture all key features of the real flow with accuracy sufficient for the needs of mine ventilation practices.

## Acknowledgment

Present work was supported by the Grant AGH No. 11.11.210.312.

## References

1. M. Jaszczur, R. Nowak, J. Szmyd, M. Branny, M. Karch, W. Wodziak, *JPCS* **318,** 052043 (2011)
2. S.M. Aminossadati, K. Hooman, *12th U.S/North AMVS* (2009)
3. B. Kuan, W. Yang, M.P. Schwarz, *Chemical Engineering Science* **62**, 2068–2088 (2007)
4. R. Mossad, W. Yang, M.P. Schwarz, *7th International Conference on CFD in the Minerals and Process Industries* (CSIRO, Melbourne, Australia 2009)
5. H. Nakayama, M. Hirota, K. Shinoda, S. Koide, *Thermal Science and Engineering* **13**, 17-23 (2005)
6. S.A. Silvester, PhD thesis, The University of Nottingham (2002)
7. A.M. Wala, S. Vytla, C.D. Taylor, G. Huang. *SME ME* **59** (10), 49 (2007)
8. A.M. Wala, J.R. Stoltz, J.D. Jacob, *Proceedings of the 7th IMVC*, 411-418 (2001)
9. M. Jaszczur, L. Portela, *ERCOFTAC SER.* **12**, 343-354 (2008)
10. J. Szmyd, M. Branny, M. Karch, W. Wodziak, M. Jaszczur, R. Nowak, *Arch. Min. Sci.* **58** (2), 333-348 (2013)
11. M. Branny, W. Filipek, *Arch. Min. Sci*. **53** (2), 221-234 (2008)
12. J. Krawczyk, *Arch. Min. Sci.* Monograph **2** (2007)
13. R.D. Keane, R.J. Adrian, *Appl. Sci. Res.* **49** (3), 191-215 (1992)
14. R.J. Adrian, *Exp. Fluids* **39** (2), 159-169 (2005)
15. M. Raffel et al., *Particle Image velocimetry: A Practical Guide* (Springer-Verlag, 2007)
16. J. Westerweel, *Digital Particle Image Velocimetry, Theory and applications* (Delft University Press, 1993)
17. *Flow Master Manual for Davis 8.0* (LaVision Gmbh, 2007)